JOURNAL OF CATALYSIS 70, 147–159 (1981)

The Structure Sensitivity of *n*-Heptane Dehydrocyclization and Hydrogenolysis Catalyzed by Platinum Single Crystals at Atmospheric Pressure

W. D. GILLESPIE,[1] R. K. HERZ,[2] E. E. PETERSEN, AND G. A. SOMORJAI

Departments of Chemistry and Chemical Engineering, University of California, Berkeley, California 94720; and Materials and Molecular Research Division, Lawrence Berkeley Laboratory, Berkeley, California 94720

Received November 4, 1980; revised January 26, 1981

The dehydrocyclization and hydrogenolysis of *n*-heptane catalyzed by platinum single-crystal surfaces have been investigated at temperatures from 533 to 603 K in the range of 1 atm total pressure. The flat (111), stepped (557), and kinked (10, 8, 7) and (25, 10, 7) surfaces used in this study were characterized under ultrahigh vacuum by low-energy electron diffraction and Auger electron spectroscopy before and after reaction experiments. The initial rate of dehydrocyclization to toluene on the four surfaces increased in the order $(111) \approx (25, 10, 7) < (557) \approx (10, 8, 7)$. Hydrogenolysis, however, increased in the order $(557) < (10, 8, 7) < (111) < (25, 10, 7)$. As a result, the selectivity of toluene production versus hydrogenolysis increased by an order of magnitude in the order $(25, 10, 7) < (111) < (10, 8, 7) < (557)$. The sum of the rates of hydrogenolysis and toluene production remains relatively constant. The effect of preoxidation of the single-crystal catalysts was to increase the rate of hydrogenolysis and decrease the rate of dehydrocyclization. In general, the reaction rates decreased with increasing reaction time. This decrease was shown to be the result of the deposition of irreversibly adsorbed carbonaceous species.

INTRODUCTION

The conversion of alkanes to cyclic molecules occurs via important, complex, and intriguing reactions which occur over suitably prepared platinum catalysts. For example, *n*-heptane can undergo dehydrocyclization to toluene, methylcyclohexane, and alkyl-cyclopentanes. Hydrogenolysis to produce light alkane fragments is one of the reactions which competes with cyclization. The structure sensitivities of these reactions have been investigated using supported (*1–8*) and thin-film (*9, 10*) catalysts of varied dispersion, single-crystal surfaces (*11, 12*), and platinum–gold alloys (*13, 14*). Although the results are not always unequivocal, these studies have generally shown that alkane hydrogenolysis and dehydrocyclization are structure-sensitive reactions, i.e., their specific rates are dependent on particle size, single-crystal surface structure, or alloy composition.

Kraft and Spindler (*1*), and Maat and Moscou (*2*) have reported that over alumina-supported platinum catalysts, the specific rate of *n*-heptane dehydrocyclization to toluene increases with decreasing particle size. The structure sensitivity of C_6 alkane dehydrocyclization has been studied in more detail than C_7 cyclization. Both methylcyclopentane and benzene can be formed from hexane and hexane isomers over platinum catalysts. In addition to being a dehydrocyclization product, methylcyclopentane is an important intermediate in one type of skeletal isomerization of hexanes (*15*). Experiments by Gault and co-workers (*5, 6*) indicate that C_5-cyclic isomerization is the dominant alkane isomerization mechanism over highly dispersed

---

[1] Present address: Shell Development Company, P.O. Box 1380, Houston, Texas 77001.

[2] Present Address: Physical Chemistry Department, General Motors Research Laboratories, Warren, Mich. 48090.

0021-9517/81/070147-13$02.00/0

catalysts, while bond shift isomerization is more important over poorly dispersed catalysts. It was concluded (*16*) that cyclization may require only one metal center. Likewise, Anderson and co-workers (*9*, *10*) used platinum films of varied dispersion to catalyze the reactions of several C_6 alkanes and found that cyclic isomerization and cyclic reaction products were favored over the most highly dispersed films. On the other hand, Dautzenberg and Platteeuw (*3*, *4*) have reported that the rates of isomerization and dehydrocyclization of *n*-hexane and 2-methylpentane are independent of particle size over monofunctional supported platinum catalysts. Van Schaik *et al.* (*14*), using a series of Pt–Au alloys of varied composition, observed a maximum in selectivity for *n*-hexane dehydrocyclization on intermediate-dispersion (intermediate platinum concentration) catalysts. The surfaces of these alloys should be composed mainly of very small ensembles of platinum atoms embedded in an inert matrix of gold atoms. These results indicate that probably only one or two platinum atoms are required to form an active site for dehydrocyclization. Kozlov *et al.* (*8*) also concluded that the specific rates of *n*-hexane dehydrocyclization were highest over intermediate-sized platinum particles dispersed on nonacidic supports.

Alkane hydrogenolysis has generally been shown to be a structure-sensitive reaction over transition metal catalysts (*8*, *9*, *17*, *18*). The specific hydrogenolysis rates of neopentane, *n*-hexane, and 2-methylpentane have been found to increase with increasing platinum dispersion over supported (*7*) and metal film catalysts (*9*, *10*).

Structure sensitivity studies using supported or thin-film catalysts are difficult to interpret because of the complex surface structure of this form of catalyst and the difficulty of determining the surface structure experimentally. While particle size effects cannot easily be assigned to specific surface sites, these effects may be applied directly to the optimization of industrial catalyst formulations. Oriented films may have substantial uncontrolled concentrations of surface defects.

Single-crystal catalysts offer the distinct advantage of allowing direct determination of the structure and composition of the active surface. Somorjai and co-workers (*11*, *12*) have used platinum single crystals to catalyze the dehydrocyclization of *n*-heptane to toluene at pressures less than 10^{-4} Torr. A flat (111) surface and several stepped surfaces with (111) terraces of varied width were used. As the terrace width was varied, a maximum in activity was observed for the (557) surface which has six-atom-wide terraces. This surface was several orders of magnitude more active than the (111) surface or a stepped surface with four-atom-wide terraces.

The present study has utilized well-characterized platinum single-crystal surfaces of varied structure to catalyze the dehydrocyclization and hydrogenolysis of *n*-heptane at pressures in the range of 1 atm. The single crystals were characterized by Auger electron spectroscopy (AES) and low-energy electron diffraction (LEED) prior to, and immediately after reaction studies. The high-pressure catalytic experiments were conducted by using a specially constructed isolation cell inserted in the center of an ultrahigh vacuum chamber. The effect of catalyst surface structure on catalytic activity, selectivity, and stability has been determined. In addition, the effect of the presence of strongly bound subsurface oxygen on catalyst performance has been explored.

EXPERIMENTAL

The experimental apparatus and procedures used here are the same as described in detail previously (*19*). The single-crystal platinum catalysts were prepared and characterized under ultrahigh vacuum, and reaction studies were performed using an isolation cell housed within the main vacuum chamber. AES and LEED were used for surface characterization before and immediately after reaction studies.

The four platinum surfaces used in this study are the (111), (557), (10, 8, 7), and (25, 10, 7) in simple Miller index notation, or more illustratively, the Pt(111), Pt(S) - $[5_5(111) + 2_1(100)]$, Pt(S) - $[7_{14}(111) + 1_1(110) + 2_2(100)]$, and the Pt(S)-$[7_{14}(111) + 15_{15}(100) + 3_3(110)]$ in microfacet notation (*20*). Idealized schematic representations of these surfaces are presented in Fig. 1. The (111) surface is a hexagonally closed packed array of atoms. The (557) crystal face is a stepped surface consisting of six-atom-wide terraces of (111) orientation separated by highly unsaturated one-atom-high steps. The other two surfaces have high concentrations of kink sites in the steps which are even more highly unsaturated than step atoms. The (10, 8, 7) surface has approximately seven-atom-wide terraces, and steps of (310) orientation, resulting in a density of kink sites of about 6% of the total surface atom concentration. The (25, 10, 7) surface has (610) orientation steps, two-atom-wide terraces, and a kink surface concentration of about 9%. These surfaces appear to be structurally stable under the conditions of the experiments reported here. The *n*-heptane was obtained from Phillips Petroleum Company and was 99.99% pure, with 2-methylhexane and 3-methylhexane as the major impurities.

The single-crystal surfaces were cleaned under vacuum prior to reaction studies by argon ion bombardment and annealing, oxygen treatments at elevated temperatures and annealing, or a combination of these two techniques. Oxidized platinum surfaces were prepared by heating the crystal in 5×10^{-7} to 5×10^{-6} Torr oxygen at temperatures of 1023–1123 K for various time periods. The calibration of surface carbon coverages developed by Biberian and Somorjai has been used throughout the present study (*25*).

Some of the experiments reported were performed in a second high-pressure reac-

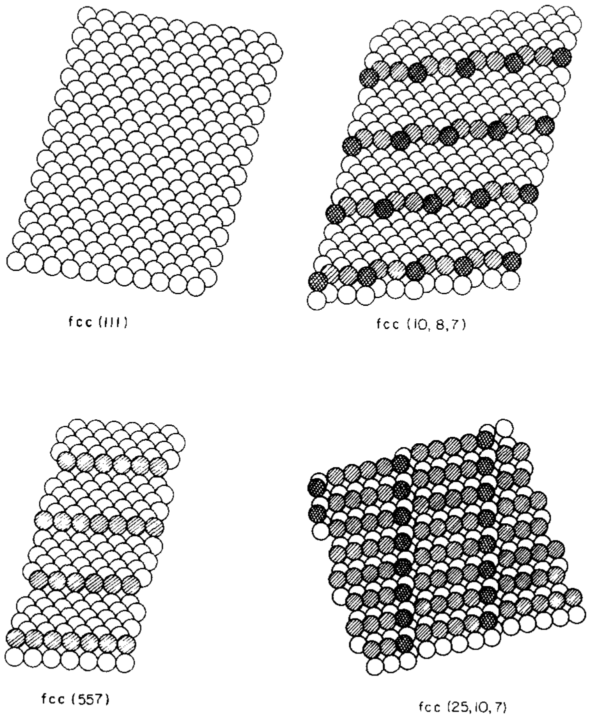

fcc (111)

fcc (10, 8, 7)

fcc (557)

fcc (25, 10, 7)

FIG. 1. Idealized representations of the single-crystal surfaces used in our reaction studies.

tion-surface analysis apparatus described in detail elsewhere (*21*). The Auger spectrometer used in this apparatus used a nonstandard flat grid arrangement (*22*). As a result, the AES calibration for surface carbon used in the primary system is not applicable to the second apparatus. Carbon coverage data from this second system will be reported in terms of arbitrary units. Unless otherwise specified, the results presented will be from the primary apparatus.

AES analysis subsequent to reaction studies did not indicate any impurities on the platinum surfaces other than carbon in the clean-surface experiments, and carbon and oxygen in the oxidized-surface experiments. Contamination by sulfur was considered a potential problem. As a result, the AES signal at 150 eV was carefully monitored in order to ensure that sulfur levels were below the AES detection limit. Oxidation of the single-crystal surfaces would occasionally result in the segregation of Ca and Si to the surface. However, when this occurred the crystal was subjected to several ion bombardment–oxidation cycles until the contamination was below AES detection limits.

RESULTS

The Initial Rates of n-Heptane Dehydrocyclization and Hydrogenolysis

Reaction studies have been performed at 15 Torr *n*-heptane, 480 to 745 Torr hydrogen, and temperatures of 533 to 603 K. Toluene, and C_1 through C_6 hydrogenolysis fragments were the only reaction products studied in detail. As a result of the low conversions ($<0.02\%$) alkyl-cyclopentanes and methylcyclohexane could not be effectively separated from *n*-heptane using our gas chromatographic method. The C_1 through C_6 alkanes have been summed and are considered collectively as the products of hydrogenolysis. These have been calibrated such that 1 mole of light alkanes produced represents 1 mole of *n*-heptane consumed. Data obtained at 15 Torr *n*-heptane, 480 Torr hydrogen, and 573 K are depicted in Figs. 2 and 3. These plots represent the accumulation of product in the batch reactor as a function of time. As a result, the rate of the reaction at any given time is the slope of the curve at that time. Table 1 lists the initial rates based on these data. Multiple data for the various surface structures are included to demonstrate the degree of reproducibility of the results. The first entry for the (10, 8, 7) crystal and the first two entries for the (111) crystals represent runs in which the crystal was prepared by sputter anneal cycles only. The remainder of the runs utilized oxidation–anneal-type cleaning procedures. The second entries for the (557) and (25, 10, 7) surfaces were obtained in the second reactor sys-

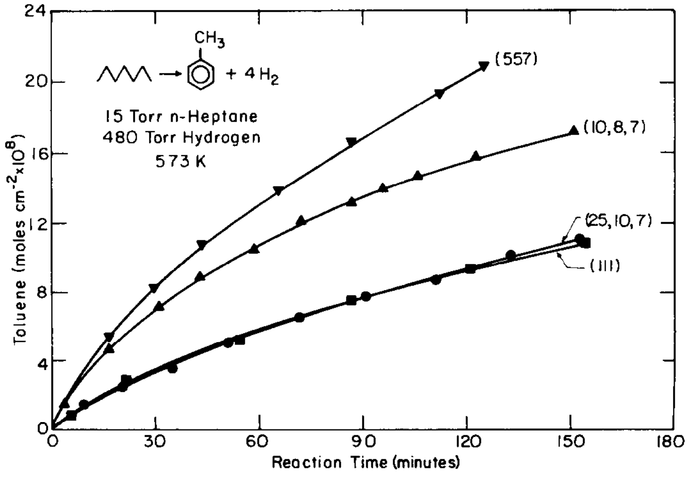

FIG. 2. Toluene formation from *n*-heptane over the four single-crystal surfaces.

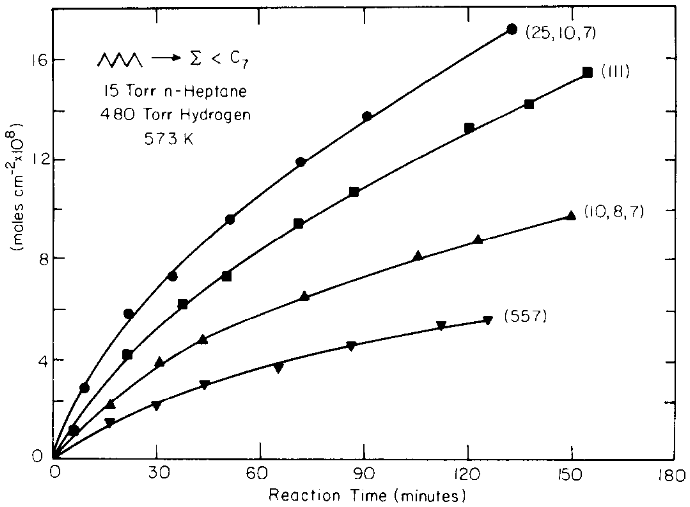

FIG. 3. *n*-Heptane hydrogenolysis over the four single-crystal surfaces.

tem. Although the rates were somewhat lower in the second system than in the first, the relative activities of the two surfaces agree quite well between the two sets of data. The initial rates were reproducible to within ±15%. Also listed in Table 1 are the selectivities, defined as the rate of toluene production divided by the rate of hydrogenolysis, and the total rate defined as the sum of the initial hydrogenolysis plus dehydrocyclization rates. Figure 4 illustrates the structure dependencies of the intial rates and selectivities. The initial rate of toluene production varied by about a factor of 2.5 and was highest on the (557) and (10, 8, 7) stepped surfaces. On the other hand, the rate of hydrogenolysis varied by a factor of 5 with a minimum on the (557) surface and a maximum on the narrow terrace, high-kink-density (25, 10, 7) surface. The selectivity

TABLE 1

Structure Dependence of Initial Rates and Selectivity at 15 Torr *n*-Heptane, 480 Torr Hydrogen, and 573 K

Surface[a]	Dehydrocyclization	Hydrogenolysis	Total rate	Selectivity[b]
	Initial rates (moles n-C_7 cm^{-2} min^{-1} × 10^{9})			
$(111)_1$[c]	1.1	1.7	2.8	0.6
$(111)_2$[c]	1.3	1.9	3.2	0.7
$(111)_2$	1.3	2.0	3.3	0.7
$(557)_1$	2.6	0.6	3.2	4.6
$(557)_2$[d]	2.0	—	—	—
(10, 8, 7)[c]	2.6	1.7	4.3	1.5
(10, 8, 7)	2.9	1.4	4.3	2.1
(10, 8, 7)	2.7	1.3	4.0	2.1
(25, 10, 7)	1.2	2.7	3.9	0.4
(25, 10, 7)[d]	1.0	—	—	—

[a] The subscripts identify different crystal samples.

[b] Initial rate of dehydrocyclization divided by the initial rate of hydrogenolysis.

[c] Crystal was cleaned only by sputtering and annealing.

[d] Data obtained in second reactor system.

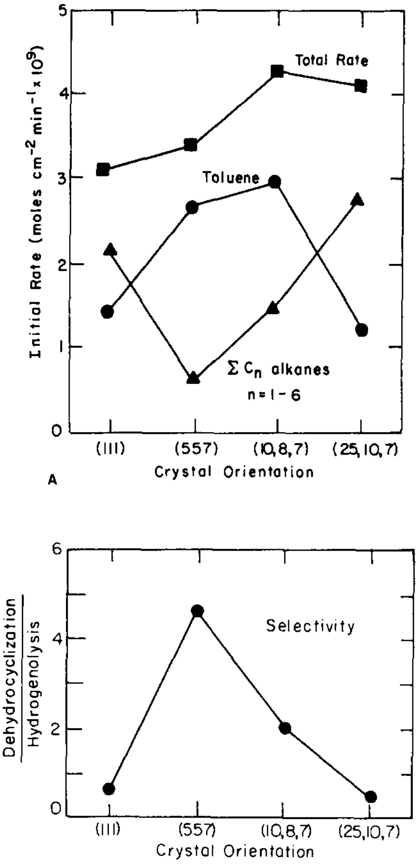

FIG. 4. The dependence of (A) initial rates and (B) selectivities at 15 Torr n-heptane, 480 Torr hydrogen, and 573 K.

varied by about a factor of 10 and was highest on the (557) surface and lowest on the (25, 10, 7) surface. As illustrated in Fig. 4, the sum of the two reactions, dehydrocyclization and hydrogenolysis, was relatively independent of surface structure. This suggests that these two reactions compete with one another. An increase in the rate of hydrogenolysis may lead to a decrease in the rate of dehydrocyclization, and vice versa.

Table 2 lists the initial rates and selectivities as a function of reaction temperatures and hydrogen pressure on the (10, 8, 7) and (111) crystal surfaces. The apparent activation energy for toluene formation was 30 ± 4 kcal/mole on the (10, 8, 7) surface and 33.6 ± 2 kcal/mole on the (111) surface. The data point at 603 K was not used to calculate the activation energies on the (10, 8, 7) surface since rapid deactivation at this temperature resulted in a large uncertainty in the initial rate measurements. The apparent activation energy for hydrogenolysis on the (10, 8, 7) surface was 14 ± 2 kcal/mole and on the (111) was 18.6 ± 2 kcal/mole. As a result, below 573 K, the selectivity for toluene production increased with increasing temperature. Increasing the hydrogen pressure increased both the rates of hydrogenolysis and dehydrocyclization.

TABLE 2

The Effect of Temperature and Hydrogen Pressure on the Initial Rates and Selectivity at 15 Torr n-Heptane

Temperature (K)	Hydrogen pressure (Torr)	Dehydrocyclization	Hydrogenolysis	Total rate	Selectivity
		Initial rates (moles n-C_7 cm^{-2} min^{-1} × 10^{-9})			
		(10, 8, 7)			
603	480	4.7	3.1	7.8	1.5
573	480	2.9	1.4	4.3	2.1
553	480	1.5	1.1	2.6	1.4
533	480	0.50	0.66	1.2	0.8
573	745	3.9	2.0	5.9	2.1
		(111)			
573	480	1.4	2.0	3.4	0.7
563	480	0.78	1.6	2.4	0.5
533	480	0.15	0.60	0.75	0.3

Deactivation and Carbonaceous Deposits

AES measurements subsequent to reaction studies indicate that 0.5 monolayer to nearly 1 monolayer of carbonaceous material is deposited on the surface under reaction conditions. Since AES is performed under vacuum, these measurements represent carbonaceous species that are irreversibly adsorbed; that is, species which are not removed from the surface upon evacuation of the reactor. It is likely that at high pressure significant concentrations of reversibly adsorbed species also exist on the catalyst surface. As a result, these measured surface carbon concentrations are probably lower than is the case under actual reaction conditions.

This irreversibly adsorbed carbonaceous deposit is quite strongly bound to the surface. Heating the crystal under vacuum or in hydrogen (760 Torr) would not remove this carbon from the surface. Generally, oxidative or sputtering treatments were necessary for this purpose. After a reaction experiment, the LEED pattern from the crystal surface contained only the diffraction features of the clean surface with a high background intensity. This indicates that within the coherence width of the electron beam the carbon does not form an ordered overlayer structure. There was no evidence from LEED that this carbon was graphitized.

The amount of hydrogen contained in the carbonaceous overlayer (irreversibly adsorbed) was estimated by thermal desorption spectroscopy (TDS). Shown in Fig. 5 are TDS spectra of H_2 from (1) the carbonaceous overlayer deposited during a high-pressure reaction experiment, (2) a layer of benzene adsorbed at 10^{-8} Torr and room temperature, and (3) hydrogen adsorbed on a clean surface at 200 Torr and room temperature. Thermal desorption of benzene from platinum generally results in no more than 10% of the carbon being removed from the surface. Rather, the benzene decomposes yielding the hydrogen TDS shown in Fig. 5. Likewise, only thermal desorption of H_2 could be detected from the reaction-deposited overlayer. By using the quantitative determination of surface carbon by AES, the hydrogen TDS can be calibrated relative to the carbon by assuming that the benzene decomposes totally, and all of the hydrogen is removed from the surface during the flash. By using the AES data for the carbon coverage in each case, and assuming a stoichiometry of one hydrogen atom per carbon atom in the benzene overlayer (i.e., associative adsorption of benzene), a ratio of one hydrogen atom per two carbon atoms in the layer deposited during reaction can be calculated. This H/C ratio of 0.5 should be considered as an upper limit since the nonvalidity of any of the three assumptions mentioned above would likely result in a lower ratio. Hydrogen thermal desorption from the reaction-deposited overlayer was not systematically studied as a function of reaction conditions or preoxidation treatment.

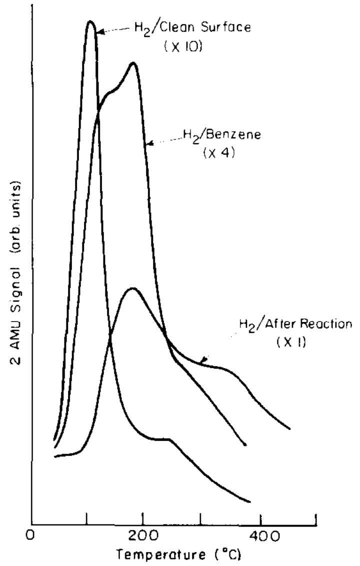

FIG. 5. Thermal desorption curves of hydrogen from the (10, 8, 7) surface with various adsorbates. For benzene and the reaction-deposited layer the carbon coverages were 0.22 and 0.74 monolayers, respectively, and the relative amounts of hydrogen desorbed were 4.32 and 7.72 (arbitrary units), respectively.

Table 3 lists the carbon coverages and

TABLE 3

Carbon Coverage and Deactivation as a Function of Reaction Conditions at 15 Torr *n*-Heptane over the (10, 8, 7) Surface

Temperature (K)	Hydrogen pressure (Torr)	Carbon[a] coverage (monolayers)	Dehydrocyclization	Hydrogenolysis	Selectivity	
			Initial rate/final rate[a]		Initial	Final[a]
603	480	0.92	15.7	1.5	1.5	0.5
573	480	0.81	5.5	3.7	2.0	1.4
553	480	0.74	2.3	3.3	1.4	1.9
533	480	0.56	1.8	3.1	0.8	0.8
573	745	0.76	5.1	2.5	2.0	1.7

[a] At 2 h of reaction time.

deactivation behavior of the (10, 8, 7) surface as a function of reaction conditions. The ratio of the initial rate versus the rate after 2 h of reaction is used as a measure of deactivation. A larger ratio indicates a greater amount of deactivation. Increasing the reaction temperature resulted in the deposition of more carbon and a higher rate of deactivation. Increasing the hydrogen pressure yielded less carbon deposition and less deactivation.

Several experiments were performed to further explore the deactivation behavior of the single-crystal catalysts. In order to eliminate inhibition by the aromatic product as the cause of deactivation, a separate experiment was performed in which 8.7 Torr of benzene was added to the normal reaction mixture at the start of an *n*-heptane reaction run. Benzene should produce inhibition effects similar to toluene, and is readily separable from toluene by gas chromatography, thus allowing the accurate determination of the rate of toluene production in the presence of a large concentration of another aromatic compound. In the presence of benzene, the initial rates of dehydrocyclization and hydrogenolysis on the (10, 8, 7) surface were 2.8×10^{-9} and 1.9×10^{-9} moles n-C_7/min-cm^2, respectively. Comparison to the rates presented in Table 1 reveals that the rate of toluene production is unchanged by the addition of benzene, while the hydrogenolysis rate may actually have been enhanced somewhat.

An attempt was made to follow the carbon deposition process with time during a reaction, and to correlate carbon coverage with deactivation. A series of six experiments was performed under the same conditions, but for varying lengths of time. Table 4 lists the results of these experiments which were performed in the second reactor system. Since the spectrometer used for AES measurements in this apparatus was not calibrated for carbon in a manner similar to the primary apparatus, the carbon coverages reported in Table 4 are in arbitrary units. Figure 6 is a plot of the relative rate (rate at a given time divided by the initial rate) versus the amount of deposited surface carbon determined at each of the times in Table 4. The second set of points in this figure are the relative rates and carbon coverages at the end of several experiments on the same crystal under var-

TABLE 4

Correlation of Carbon Coverage and Deactivation over the (557) Surface

Time (min)	Carbon coverage (arbitrary units)	Relative rate[a]
1.5	0.4	0.26
4	0.6	0.088
25	1.0	0.016
60	1.1	0.007
240	1.4	0.004

[a] Rate at the time of the carbon coverage measurement divided by the initial rate.

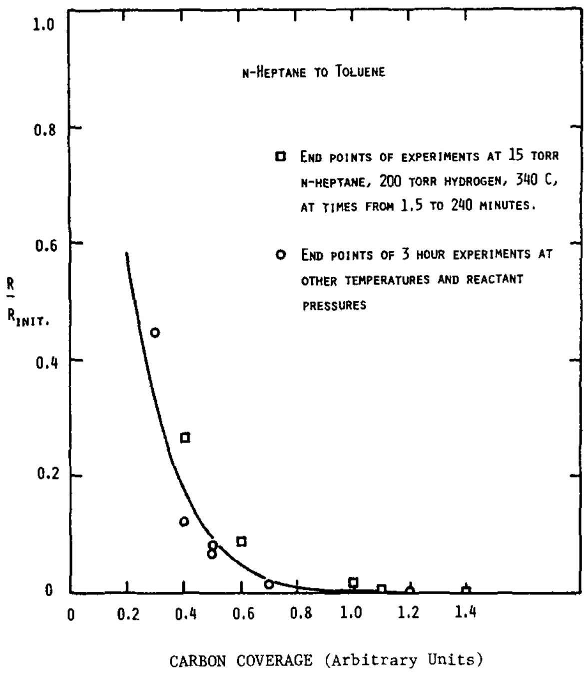

FIG. 6. Correlation of the deactivation of *n*-heptane aromatization with carbon coverage over the (557) surface.

ious other temperature and pressure conditions.

In summary, these results show that the deactivation which occurs during a run is the result of the deposition of irreversibly adsorbed carbonaceous species. Reaction inhibition by the aromatic product is not significant. The rate of carbon deposition and the rate of deactivation increase with increasing temperature and decreasing hydrogen pressure.

Table 5 lists the carbon coverages and deactivation as a function of surface structure. Carbon deposition did not depend strongly on surface orientation. The rate of deactivation of toluene production varied by about a factor of 3 with changes in surface structure, but did not exhibit an obvious trend with crystal face. Hydrogenolysis deactivation was rather insensitive to surface structural variations. The selectivity for toluene production increased with

TABLE 5

Carbon Coverage and Deactivation as a Function of Surface Structure at 15 Torr *n*-Heptane, 480 Torr Hydrogen, and 573 K

Surface structure	Carbon[a] coverage (monolayers)	Dehydrocyclization	Hydrogenolysis	Selectivity	
		(Initial rate/final rate[a])		Initial	Final[a]
(111)	0.6	4	3.2	0.7	0.5
(557)	0.6	3.3	2.4	4.6	3.2
(10, 8, 7)	0.8	5.8	3.3	2.0	1.2
(25, 10, 7)	0.7	1.9	2.9	0.4	0.7

[a] At 2 h of reaction time.

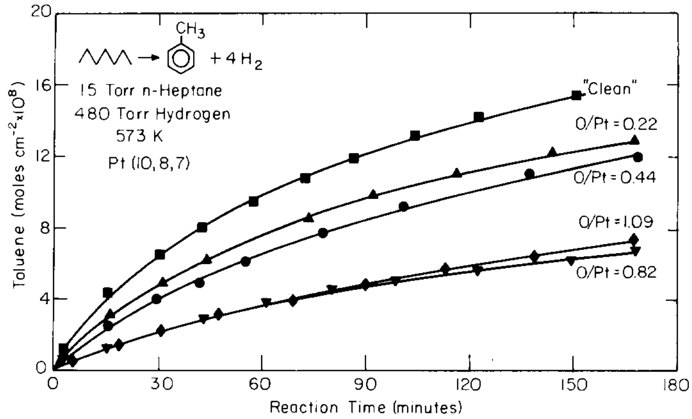

FIG. 7. The effect of preoxidation of the (10, 8, 7) surface on *n*-heptane dehydrocyclization.

reaction time over the (25, 10, 7) surface, but decreased with time over the other three orientation surfaces.

The Effect of Strongly Bound Subsurface Oxygen on Catalytic Selectivity

The effects of preoxidation of the (10, 8, 7) surface on dehydrocyclization and hydrogenolysis are illustrated by the data in Figs. 7 and 8, and Table 6. The O_{510}/Pt_{237} ratios are the initial AES ratios. In general, the intensity of the O_{510} Auger peak decreased by no more than 20% during a 2-h high-pressure reaction experiment. As the initial surface oxygen concentration on this surface was increased, the rate of hydrogenolysis increased and the rate of dehydrocyclization decreased. As a result, the selectivity changed by a factor of 20, while the total rate changed by a factor of 2. The deactivation behavior of the single-crystal catalysts was, in general, not affected significantly by the presence of the oxide. An exception to this can be seen in Fig. 8 for an initial oxygen coverage of $O_{510}/Pt_{237} = 0.82$. In this case the hydrogenolysis activity decreased more rapidly than in any of the other runs. AES analysis after this experiment revealed that the oxygen concentration had decreased by about 40%. Apparently some of the oxygen initially present was bound less

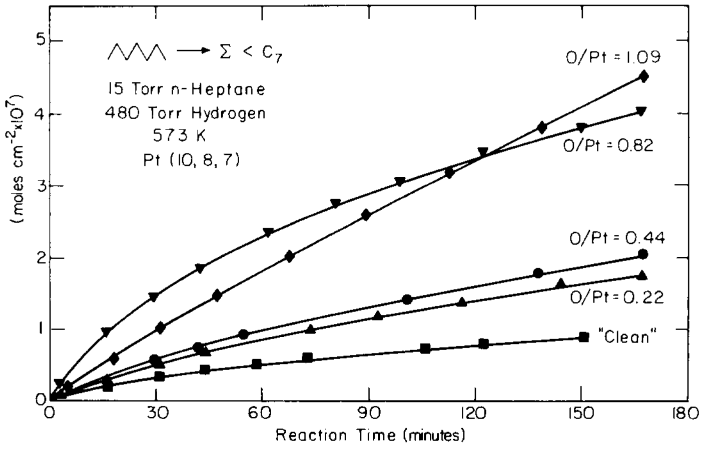

FIG. 8. The effect of preoxidation of the (10, 8, 7) surface on *n*-heptane hydrogenolysis.

TABLE 6

The Effect of Preoxidation on Initial Rates and Selectivity at 15 Torr *n*-Heptane, 480 Torr Hydrogen, and 573 K

O_{510}/Pt_{237}	Dehydrocyclization	Hydrogenolysis	Total	Selectivity
	Initial rates (moles n-C_7 cm^2 × 10^9)			
	(25, 10, 7)			
0	1.2	2.7	3.9	0.4
0.34	0.69	3.0	3.7	0.2
1.10	0.64	2.8	3.4	0.2
1.73	0.77	3.6	4.4	0.2
2.34	0.52	2.4	2.9	0.2
	(10, 8, 7)			
0	2.7	1.4	4.1	1.9
0.22	2.4	2.6	5.0	0.9
0.44	1.7	2.6	4.3	0.7
0.82	1.0	7.6	8.6	0.1
1.09	0.91	4.1	5.0	0.2

strongly than usual and was more reactive with the reaction mixture. It is unknown at the present time why this occurred since the pretreatment procedure had not been altered.

Also listed in Table 6 is the data for the oxygen effect on the selectivity of the (25, 10, 7) surface. In this case the selectivity only changed by a factor of 2. Figure 9 is a plot of the normalized selectivities (the selectivity divided by the selectivity of the clean surface) versus the surface oxygen concentration on the (557), (10, 8, 7), and (25, 10, 7) surfaces. In all cases the selectivity for toluene production decreased upon oxidation of the crystal. The magnitude of the effect decreased in the order (10, 8, 7) > (557) > (25, 10, 7). Data for the effect of oxygen on the (111) surface were not obtained.

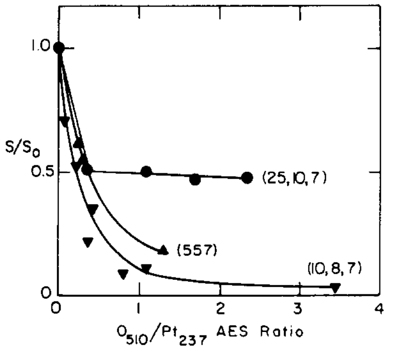

FIG. 9. Normalized selectivities as a function of surface oxygen concentration.

DISCUSSION

Examination of the data in Tables 1 and 6 reveals that under constant reaction conditions, the selectivity can change significantly as a function of catalyst properties, while the sum of the rates of hydrogenolysis plus toluene production remains relatively constant. For example, in Table 1 the selectivity changes by approximately a factor of 12 as the total rate varies only by a factor of 1.3. This suggests that the two reactions do not occur independently, and that a common slow step precedes the reaction steps which regulate the selectivity. Not enough molecular structural information exists at this time to propose a detailed mechanism that explains these observations. However, it does appear that the two reaction pathways branch from a common intermediate which has a limited surface concentration. The following reaction scheme might be applicable to this situation:

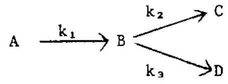

where $k_1 < k_2, k_3$. A change in either k_2 or k_3 would not cause a change in the overall rate, but would result in a change in selectivity. If, for example, k_2 increases while k_3 remains constant, the rate of formation of C would increase and the rate of formation of D would necessarily decrease. The real situation is certainly more complicated than this simple picture. For example, other reaction pathways, such as isomerization and cyclization to five-membered rings have not been included. However, this model provides a convenient picture of some aspects of the observed kinetic behavior. It seems that it is this competitive nature of the two reactions that is responsible for the complexity (the nonmonotonic dependence on step or kink density) of the structurally dependent changes in the rates of hydrogenolysis and toluene production over the single-crystal catalysts.

The selectivity for cyclization is highest on the (557) and (10, 8, 7) surfaces. Both of these surfaces have steps separated by six- to seven-atom-wide terraces. The selectivity is low on the (111) surface which does not have steps, and is also low on the (25, 10, 7) surface which has closely spaced steps. We conclude from these results that steps separated by six- to seven-atom-wide terraces, or the combination of a step and a six- to seven-atom-wide terrace, is a structure that effectively catalyzes cyclization. Assuming that step and kink sites adsorb hydrocarbons more strongly than do (111)-type sites, the close spacing of the steps on the (25, 10, 7) surface may increase the probability of simultaneous adsorption of the *n*-heptane molecule at two different points on the surface. This multiple attachment may hinder cyclization and enhance hydrogenolysis. Interestingly, the separation between the steps on the (557) and (10, 8, 7) surfaces is greater than the length of an *n*-heptane molecule. Since the (111) surface contains few step sites, we can understand why the cyclization rate is low over this surface, but were surprised that the hydrogenolysis rate is high. However, the competitive reaction model discussed above suggests that a low probability for cyclization should result in a high hydrogenolysis rate.

The major difference between the (557) and (10, 8, 7) surfaces is the presence of a kink every third atom along the steps on the (10, 8, 7) surface. The addition of kinks to steps apparently increases the rate of hydrogenolysis relative to cyclization. The (25, 10, 7) surface has only 50% more kink sites than the (10, 8, 7) surface, while its selectivity is five times lower. Thus the low selectivity of the (25, 10, 7) surface does not correlate directly with the surface kink atom concentration and must be related to the close spacing of the steps on this surface.

Earlier studies (*11*, *12*) on single-crystal platinum surfaces at low pressure (10^{-5} Torr) did not measure hydrogenolysis rates, but did determine the effect of surface structure on the rate of *n*-heptane dehydrocyclization. Over a series of stepped surfaces similar to those used in the present study, the rate of toluene production exhibited a maximum as a function of terrace width. In good agreement with the present study, the maximum occurred over the (557) surface with six-atom-wide terraces. Kinked surfaces were not included in the low-pressure study.

As demonstrated by the data in Fig. 6, the extent of deactivation of the (557) surface correlated with increasing surface carbon concentration. However, the exact dependence of deactivation on surface carbon coverage is not the same from crystal face to crystal face. That is, a given amount of carbon does not produce the same degree of deactivation on each different surface orientation. Also, the effect of carbon deposition on the selectivity was a function of surface structure. Over the (25, 10, 7) surface the selectivity increased as the crystal deactivated, while over the other three surfaces the selectivity decreased with crystal deactivation. These results suggest that in addition to the concentration of surface carbon, the structure and/or composition of the carbonaceous deposit may also be important in regulating selectivity changes and deactivation behavior of the single-crystal catalysts. No information in this regard could be obtained by LEED or AES.

Preoxidation of the single-crystal catalysts generally resulted in an increase in the selectivity of hydrogenolysis versus dehydrocyclization. Possible models of how this preoxidation could affect platinum-catalyzed hydrocarbon reactions have been discussed in detail previously (*23*, *24*). It was concluded that the main effect of preoxidation is to modify the electronic properties of the surface such that the platinum atoms become electron deficient. The actual mechanism of how this change in electronic properties alters the cyclization/hydrogenolysis selectivity is not known at present. However, it can be suggested that this change in selectivity is related to the strength of interaction between the adsorbed hydrocarbon species and the platinum surface. Strong Pt–C bonds would be expected to favor C–C bond-breaking processes. Possibly, stronger Pt–C bonds form on an oxidized surface as opposed to a nonoxidized platinum surface as a result of increased electron transfer from the hydrocarbon molecules to the surface.

ACKNOWLEDGMENT

This work was supported by the Division of Materials Science, Office of Basic Energy Sciences, U.S. Department of Energy under Contract W-7405-ENG-48 and by the U.S. Department of the Army.

REFERENCES

1. Kraft, M., and Spindler, H., *in* "Proceedings, 4th International Congress on Catalysis, Moscow, 1968" (B. A. Kazansky, Ed.), paper 69. Adler, New York, 1968.
2. Maat, H. J., and Moscou, L., *in* "Proceedings, 3rd International Congress on Catalysis, Amsterdam, 1964," p. 1278. Wiley, New York, 1965.
3. Dautzenberg, F. M., and Platteeuw, J. C., *J. Catal* **24,** 364 (1972).
4. Dautzenberg, F. M., and Platteeuw, J. C., *J. Catal.* **19,** 41 (1970).
5. Corolleur, C., Gault, F. G., Juttard, O., Maire, G., and Muller, J. M., *J. Catal.* **27,** 466 (1967).
6. Maire, G., Coroleur, C., Juttard, D., and Gault, F. G., *J. Catal.* **21,** 250 (1971).
7. Boudart, M., Aldag, A. W., Ptak, L. D., and Benson, J. E., *J. Catal.* **11,** 35 (1968).
8. Kozlov., N. S., Ivan'Kovech, E. F., Nolkodatov, A. F., and Zhizhenko, G. A., *Kinet. Katal.* **14,** 1550 (1973).
9. Anderson, J. R., Macdonald, R. J., and Shimoyama, Y., *J. Catal.* **20,** 147 (1971).
10. Anderson, J. R., and Shimoyama, Y., *in* "Proceedings, 5th International Congress on Catalysis, Palm Beach, 1972" (J. W. Hightower, Ed.), paper 47. North-Holland, Amsterdam, 1973.
11. Joyner, R. W., Lang, B., and Somorjai, G. A. *J. Catal.* **27,** 405 (1972).
12. Blakely, D. W., Ph.D. dissertation, University of California, Berkeley, 1976.
13. O'Cinneide, A., and Gault, F. G., *J. Catal.* **37,** 311 (1975).
14. Van Schaik, J. R. H., Dessing, R. P., and Ponec, V., *J. Catal.* **38,** 273 (1975).
15. Barron, Y., Coronet, D., Maire, G., and Gault, F. G., *J. Catal.* **2,** 152 (1963).
16. Muller, J. M., and Gault, F. G., *J. Catal.* **24,** 361 (1972).
17. Yates, D. J. C., Taylor, W. F., and Sinfelt, J. H., *J. Amer. Chem. Soc.* **86,** 2996 (1964).
18. Yates, D. J. C., and Sinfelt, J. H., *J. Catal.* **8,** 348 (1967).
19. Herz, R. K., Gillespie, W. D., Petersen, E. E., and Somorjai, G. A., *J. Catal* **67,** 371 (1981).
20. Van Hove, M. A., and Somorjai, G. A., *Surface Sci.* **92,** 489 (1980).
21. Kahn, D. R., Petersen, E. E., and Somorjai, G. A., *J. Catal.* **34,** 294 (1974).
22. Herz, R. K., Ph.D. dissertation, University of California, Berkeley, 1977.
23. Gillespie, W. D., Ph.D. dissertation, University of California, Berkeley, 1980.
24. Smith, C. E., Biberian, J. P., and Somorjai, G. A., *J. Catal.* **57,** 426 (1979).
25. Biberian, J. P., and Somorjai, G. A., *Appl. Surface Sci.* **2,** 352 (1979).